

Stability of micropolar fluid flow between concentric rotating cylinders

HUEI CHU WENG¹, CHA'O-KUANG CHEN²†
AND MIN-HSING CHANG³

¹Department of Mechanical Engineering, Chung Yuan Christian University,
Chungli 32023, Taiwan, ROC

²Department of Mechanical Engineering, National Cheng Kung University, Tainan 70101, Taiwan, ROC

³Department of Mechanical Engineering, Tatung University, Taipei 10452, Taiwan, ROC

(Received 7 April 2008 and in revised form 16 March 2009)

In this study, the theory of micropolar fluids is employed to study the stability problem of flow between two concentric rotating cylinders. The field equations subject to no-slip conditions (non-zero velocity and microrotation velocity components) at the wall surfaces are solved. The analytical solutions of the velocity and microrotation velocity fields as well as the shear stress difference, couple stress and strain rate for basic flow are obtained. The equations with respect to non-axisymmetric disturbances are derived and solved by a direct numerical procedure. It is found that non-zero wall-surface microrotation velocity makes the flow faster and more unstable. Moreover, it tends to reduce the limits of critical non-axisymmetric disturbances. The effect on the stability characteristics can be magnified by increasing the microstructure or couple-stress parameter or the microinertia parameter for the cases of corotating cylinders and a stationary outer cylinder or by decreasing the radius ratio or the microinertia parameter for the case of counterrotating cylinders.

1. Introduction

The theory of microfluids proposed by Eringen (1964) deals with a class of non-Newtonian fluids which exhibit certain microscopic effects arising from the presence of microstructure. Eringen (1966) simplified it to obtain the model of micropolar fluids by restricting the form of the gyration tensor, through which the theory of microfluids allows a wide variety of microstructure. Due to the simplicity, this model has been widely used in numerous applications of science and technology to describe the rheological behaviour of certain real fluids, such as exotic lubricants (Allen & Kline 1971; Khonsari & Brewé 1989; Khonsari 1990), colloidal suspensions (Hadimoto & Tokioka 1969; Rosenthal *et al.* 2004), liquid crystals (Eringen 1993), animal blood (Popel, Regirer & Usick 1974; Kang & Eringen 1976), water (Papautsky *et al.* 1999), etc. Excellent reviews of the literature on mathematical aspects and applications were provided by Ariman, Turk & Sylvester (1973, 1974), Lukaszewicz (1999) and Eringen (2001).

Stability problems of micropolar fluid flow are of great importance in research activities due to industrial applications of fluids with additives. Liu (1970, 1971) undertook the work and found that the presence of microstructure stabilizes plan flow.

† Email address for correspondence: ckchen@mail.ncku.edu.tw

Kuemmerer (1978) conducted a more detailed analysis for the instability of plan Poiseuille flow. Sastry & Das (1985) studied the stability of Couette flow and Dean flow. Brutyan & Krapivsky (1992) studied the stability of Kolmogorov flow. Das, Guha & Chattopadhyay (2005) implemented the stability analysis for hydrodynamic journal bearings.

We concern ourselves with the problem of Couette flow, a viscous fluid flowing in the annulus between two concentric rotating cylinders. In cylindrical polar coordinates (r, θ, z) , the appropriate velocity and microrotation velocity fields for fully developed laminar flow are of the form

$$\mathbf{u} = (u_r, u_\theta, u_z) = (0, u(r), 0), \quad \boldsymbol{\omega} = (\omega_r, \omega_\theta, \omega_z) = (0, 0, \omega(r)). \quad (1)$$

Let R_1 and R_2 be the radii of the inner and outer cylinders, and let Ω_1 and Ω_2 be their angular velocities. Ariman, Cakmak & Hill (1967) have examined the flow of micropolar fluids between a stationary inner cylinder and a concentric rotating outer cylinder with the boundary conditions

$$u(R_1) = 0, \quad u(R_2) = R_2\Omega_2, \quad \omega(R_1) = 0, \quad \omega(R_2) = 0. \quad (2)$$

They found that microstructure in fluids has a profound influence on the flow. Recently, numerous researchers have adopted the same law to study hydrodynamic journal bearings under micropolar lubrication, e.g. Wang & Zhu (2004, 2006), and concluded that the presence of microstructure increases the load capacity. Using the boundary conditions,

$$u(R_1) = R_1\Omega_1, \quad u(R_2) = R_2\Omega_2, \quad \omega(R_1) = 0, \quad \omega(R_2) = 0, \quad (3)$$

Verma & Sehgal (1968) further derived analytical solutions for the flow between two concentric rotating cylinders in a simple closed form and discussed the variations of the microrotation velocity field, shear stress difference, couple stress and strain rate with the radius for a specific material case. There was a controversy over the zero microrotation velocity condition given in (2) and (3). In order to ensure fluid particles near the walls adhere to the wall surfaces due to the physical structure of surfaces, i.e. its roughness and generally topography, Stokes (1984) re-examined the problem of Ariman, Cakmak & Hill (1967) by using the physically more suitable boundary conditions:

$$u(R_1) = 0, \quad u(R_2) = R_2\Omega_2, \quad \omega(R_1) = 0, \quad \omega(R_2) = \Omega_2. \quad (4)$$

Although the basic Couette flow of micropolar fluids under the no-slip conditions (4) has been investigated by Stokes, the work of the flow between two concentric rotating cylinders has not been done yet.

It is of both practical and technical interest to study the stability of viscous Couette flow. Taylor (1923) initiated the investigation. Krueger, Gross & Diprima (1966) carried out a complete linear stability analysis and found that, for a sufficiently negative value of the angular velocity ratio, the onset of instability is dominated by a non-axisymmetric mode. Their numerical simulations were later verified by the experiments of Andereck, Lin & Swinney (1986). Fluid effects on the flow stability have been studied extensively, e.g. in Sastry & Das (1985) for micropolar fluids, Chen & Chang (1998) for electrically conducting fluids, Chang, Chen & Weng (2003) for ferrofluids, etc. Sastry & Das studied the stabilizing influence of microstructure in fluids by using the boundary conditions (3). With the aid of the shooting method, they made a linear stability analysis and concluded that the presence of microstructure hinders the onset of instability. This research, however, neglected the effects of the

radius ratio and microinertia and assumed that the disturbances are axisymmetric modes. The stability problem of Couette flow of micropolar fluids with respect to non-axisymmetric disturbances for different values of the radius ratio and microinertia parameter should be studied extensively.

In this study, we combine the field equations of micropolar fluids with no-slip conditions ($u(R_1) = R_1\Omega_1$, $u(R_2) = R_2\Omega_2$, $\omega(R_1) = \Omega_1$, $\omega(R_2) = \Omega_2$) at the wall surfaces to solve the problem of Couette flow. Because the instability of Couette flow is of considerable interest for practical applications, a complete linear stability analysis will be particularly implemented in this study, in which three-dimensional disturbances are considered. The main purpose of this research is to examine how non-zero wall-surface microrotation velocity affects the flow and the onset of instability. The deterministic nature of the field equations is stated, and the proper formulas for the shear and vortex viscosities are provided based on available literature. A systematic study for different values of the microstructure, couple-stress and microinertia parameters at different values of the radius and angular velocity ratios is then carried out. The results obtained provide an overview of the flow and stability characteristics of this important hydrodynamics problem of micropolar fluids.

2. Problem formulations and analysis

2.1. Field equations and physical properties

In a general theory of fluids with microstructure, additional kinematic measures must be introduced to describe the internal spin of fluids for the velocity field, and couple stresses should be present for the microrotation velocity field, an average sense for the rotation of fluid particles in a small volume element. The balance principles for mass, linear momentum and angular momentum are

$$\nabla \cdot \mathbf{u} = 0, \tag{5}$$

$$\rho \frac{d\mathbf{u}}{dt} = -\nabla p + \eta \nabla^2 \mathbf{u} + 2\eta_R \nabla \times (\boldsymbol{\omega} - \widehat{\boldsymbol{\omega}}), \tag{6}$$

$$\rho \phi \frac{d\boldsymbol{\omega}}{dt} = (\alpha + \beta) \nabla \nabla \cdot \boldsymbol{\omega} + \gamma \nabla^2 \boldsymbol{\omega} - 4\eta_R (\boldsymbol{\omega} - \widehat{\boldsymbol{\omega}}), \tag{7}$$

where d/dt is the material derivative, ϕ is the moment of inertia per unit mass, $\widehat{\boldsymbol{\omega}}$ is the flow vorticity vector, related to the velocity vector \mathbf{u} by $\widehat{\boldsymbol{\omega}} = \nabla \times \mathbf{u}/2$, η is the shear viscosity, ρ is the density, p is the pressure, η_R is the vortex viscosity, α and β are the bulk spin viscosity and γ is the shear spin viscosity. Here, for simplicity, we have neglected the external force and moment and considered isothermal liquid flow, so that fluid compressibility is negligible. The companion constitutive relations of (6) and (7) are

$$\mathbf{T} = -p\mathbf{I} + 2\eta\mathbf{D} + 2\eta_R \mathbf{e} \cdot (\widehat{\boldsymbol{\omega}} - \boldsymbol{\omega}), \tag{8}$$

$$\mathbf{M} = \alpha (\nabla \cdot \boldsymbol{\omega})\mathbf{I} + \beta \nabla \boldsymbol{\omega} + \gamma (\nabla \boldsymbol{\omega})^T, \tag{9}$$

where \mathbf{T} is the stress tensor, \mathbf{M} is the couple stress tensor, $\mathbf{D} = ((\nabla \mathbf{u})^T + \nabla \mathbf{u})/2$ is the deformation rate tensor, \mathbf{I} is the Kronecker delta and \mathbf{e} is the third order alternating pseudotensor. Note that the couple stress tensor can be found in Eringen (1966). However, the stress tensor proposed by Eringen is

$$\mathbf{T} = -p\mathbf{I} + (2\eta + \eta_R)\mathbf{D} + \eta_R \mathbf{e} \cdot (\widehat{\boldsymbol{\omega}} - \boldsymbol{\omega}). \tag{10}$$

In (8), we have revised the constitutive relation by replacing $\eta + \eta_R/2$ with the shear viscosity and $\eta_R/2$ with the vortex viscosity, as shown in Stokes (1984). The resultant (6) has been extensively applied in the literature.

For a fluid containing additives, (6) relates linear momentum to the forces that act on the fluid, and (7) relates angular momentum to the moments or torques acting on the fluid. The presence of microstructure causes the collision and friction between additives (additive–additive interaction) and between additives and walls (additive–wall interaction) when it is flowing; that is, the bulk spin torque $(\alpha + \beta)\nabla\nabla \cdot \boldsymbol{\omega}$ and shear spin torque $\gamma\nabla^2\boldsymbol{\omega}$ are applied. From (7), the two spin torques lead to the deviation between the microrotation velocity and the flow vorticity and, therefore, result in an additional viscous force, reflecting in the term $2\eta_R\nabla \times (\boldsymbol{\omega} - \hat{\boldsymbol{\omega}})$ given in (6). Brenner (1970) proposed an original formula of the vortex viscosity. An improved form was used by Shliomis (1972), written as

$$\eta_R = \frac{3}{2}\eta\varphi, \quad (11)$$

where φ is the additive volume fraction. Reported experiments for the magnetoviscosity of ferrofluids have confirmed the viscosity law, e.g. by Holderied, Schwab & Stierstadt (1988) for $\varphi = 1.40 \times 10^{-1}$, Embs *et al.* (2000) for $\varphi = 8.37 \times 10^{-2}$ and Patel, Upadhyay & Mehta (2003) for $\varphi = 8.85 \times 10^{-2}$. Note that it is often necessary to consider the particle collision and friction to ensure that a magnetoviscosity expression using formula (11) is valid for different dense fluids (Ambacher, Odenbach & Stierstadt 1992; Odenbach & Gilly 1996). In addition to the additive–additive and additive–wall interactions, the viscous force could partly result from the collision and friction between additives and fluid molecules. This concept was made quantitative by Einstein (1906), who gave a simple correction to the shear viscosity η . Einstein's formula is described by

$$\eta = \eta_0(1 + 2.5\varphi), \quad (12)$$

where η_0 is the shear viscosity of the fluid without additives (carrier liquid).

The following restrictions on the micropolar material constants can be obtained from thermodynamics, providing that the Clausius–Duhem inequality is satisfied locally for all independent processes:

$$\left. \begin{aligned} \eta/K \geq 0, \quad \eta_R/K \geq 0, \quad \gamma/K \geq 0, \\ (3\alpha + 2\gamma)/K \geq 0, \quad -\gamma/K \leq \beta/K \leq \gamma/K. \end{aligned} \right\} \quad (13)$$

Here, K is the temperature and $K > 0$ is general. In this study, we introduce the dimensionless micropolar parameters that relate the shear viscosity η to the material constants as follows:

$$\eta_v = \frac{\eta_R}{\eta}, \quad \eta_s = \frac{\gamma}{\eta\bar{d}^2}, \quad \eta_b = \frac{\alpha + \beta}{\eta\bar{d}^2}, \quad (14)$$

where $\bar{d} = R_2 - R_1$ and η_v , η_s and η_b are the parameters for microstructure and couple stresses, respectively.

2.2. Basic Couette flow

In this section, we develop the mathematical model of the basic Couette flow as a basic condition of flow with disturbance. Assume that the field equations (5)–(7) admit a steady solution of the form:

$$\mathbf{u} = (u_r, u_\theta, u_z) = (0, u(r), 0), \quad p = p(r), \quad \boldsymbol{\omega} = (\omega_r, \omega_\theta, \omega_z) = (0, 0, \omega(r)). \quad (15)$$

Then, (5) is identically satisfied, and (6) and (7) are reduced to

$$(\eta + \eta_R)D'_*D'_*u - 2\eta_R D'_*\omega = 0, \tag{16}$$

$$\gamma D'_*D'_*\omega + 2\eta_R D'_*u - 4\eta_R\omega = 0, \tag{17}$$

$$D'_*p = \rho \frac{u^2}{r}, \tag{18}$$

where

$$D'_* = d/dr + 1/r, \quad D' = d/dr. \tag{19}$$

Integrating (16)–(18), we obtain

$$\left. \begin{aligned} u(r) &= \frac{2\eta_v}{1 + \eta_v} \frac{1}{k} (AI_1(kr) - BK_1(kr)) + Cr + \frac{D}{r}, \\ \omega(r) &= AI_0(kr) + BK_0(kr) + C, \\ p(r) &= \rho \int \frac{u^2}{r} dr, \end{aligned} \right\} \tag{20}$$

where

$$k = \left(\frac{\eta_v}{\eta_s (1 + \eta_v)} \right)^{1/2} \frac{2}{\bar{d}}, \tag{21}$$

I_0 , I_1 and K_0 , K_1 are the first-kind and second-kind modified Bessel functions of zeroth order and first order, and A , B , C and D are arbitrary constants.

Considering the no-slip boundary conditions

$$u(R_1) = R_1\Omega_1, \quad u(R_2) = R_2\Omega_2, \quad \omega(R_1) = \Omega_1, \quad \omega(R_2) = \Omega_2, \tag{22}$$

we obtain

$$A = \Omega_1 NS^{-1}, \quad B = -\Omega_1 OS^{-1}, \quad C = \Omega_1 PS^{-1}, \quad D = R_2^2\Omega_2 - R_2^2\Omega_1 QS^{-1}, \tag{23}$$

where

$$\left. \begin{aligned} \varepsilon &= kR_2, \quad \mu = \Omega_2/\Omega_1, \quad \zeta = R_1/R_2, \\ b &= I_1(\varepsilon) - \zeta I_1(\zeta\varepsilon), \quad c = K_1(\varepsilon) - \zeta K_1(\zeta\varepsilon), \quad d = K_0(\varepsilon) - K_0(\zeta\varepsilon), \\ e &= I_0(\varepsilon) - I_0(\zeta\varepsilon), \quad f = K_0(\varepsilon) - \mu K_0(\zeta\varepsilon), \quad g = I_0(\varepsilon) - \mu I_0(\zeta\varepsilon), \\ N &= d(\mu - \zeta^2) - f(1 - \zeta^2) - \frac{2\eta_v}{1 + \eta_v} \frac{c}{\varepsilon} (1 - \mu), \\ O &= e(\mu - \zeta^2) - g(1 - \zeta^2) + \frac{2\eta_v}{1 + \eta_v} \frac{b}{\varepsilon} (1 - \mu), \\ P &= \frac{2\eta_v}{1 + \eta_v} \frac{1}{\varepsilon} (bf + cg) + (\mu - \zeta^2) (-dI_0(\zeta\varepsilon) + eK_0(\zeta\varepsilon)), \\ Q &= \frac{2\eta_v}{1 + \eta_v} \frac{1}{\varepsilon} (NI_1(\varepsilon) + OK_1(\varepsilon)) + P, \\ S &= \frac{2\eta_v}{1 + \eta_v} \frac{1}{\varepsilon} (bd + ce) + (1 - \zeta^2) (-dI_0(\zeta\varepsilon) + eK_0(\zeta\varepsilon)). \end{aligned} \right\} \tag{24}$$

Hence, the dimensionless velocity is

$$U(\kappa) = \frac{u}{R_1\Omega_1} = \left(\frac{2\eta_v}{1 + \eta_v} \frac{1}{\zeta\varepsilon} (NI_1(\varepsilon\kappa) + OK_1(\varepsilon\kappa)) + P\kappa/\zeta - Q/\zeta\kappa \right) S^{-1} + \frac{\mu}{\zeta\kappa}, \tag{25}$$

and the dimensionless microrotation velocity is

$$\Omega(\kappa) = \frac{\omega}{\Omega_1} = (NI_0(\varepsilon\kappa) - OK_0(\varepsilon\kappa) + P) S^{-1}, \tag{26}$$

where

$$\kappa = r/R_2. \tag{27}$$

From (8) and (9), we obtain

$$\left. \begin{aligned} t_{rr} &= -p, \quad t_{r\theta} = (\eta - \eta_R) \left(\frac{du}{dr} - \frac{u}{r} \right) + 2\eta_R \left(\frac{d\omega}{dr} - \omega \right), \quad t_{rz} = 0, \\ t_{\theta r} &= (\eta - \eta_R) \left(\frac{du}{dr} - \frac{u}{r} \right) + 2\eta_R \left(-\frac{u}{r} + \omega \right), \quad t_{\theta\theta} = -p, \quad t_{\theta z} = 0, \\ t_{zr} &= 0, \quad t_{z\theta} = 0, \quad t_{zz} = -p, \end{aligned} \right\} \tag{28}$$

$$\left. \begin{aligned} m_{rr} &= 0, \quad m_{r\theta} = 0, \quad m_{rz} = \gamma \frac{d\omega}{dr}, \\ m_{\theta r} &= 0, \quad m_{\theta\theta} = 0, \quad m_{\theta z} = 0, \\ m_{zr} &= \beta \frac{d\omega}{dr}, \quad m_{z\theta} = 0, \quad m_{zz} = 0. \end{aligned} \right\} \tag{29}$$

The dimensionless shear stress difference is

$$T_{r\theta}(\kappa) = \frac{t_{r\theta} - t_{\theta r}}{\eta\Omega_1} = 4\eta_v (NI_0(\varepsilon\kappa) - OK_0(\varepsilon\kappa)) \left(\frac{\eta_v}{1 + \eta_v} - 1 \right) S^{-1}, \tag{30}$$

the dimensionless couple stress is

$$M_{rz}(\kappa) = \frac{m_{rz}}{\gamma\Omega_1/R_1} = \frac{m_{zr}}{\beta\Omega_1/R_1} = \zeta\varepsilon (NI_1(\varepsilon\kappa) + OK_1(\varepsilon\kappa)) S^{-1}, \tag{31}$$

and the dimensionless strain rate is

$$\begin{aligned} \dot{\Gamma}(\kappa) &= \frac{2\dot{\gamma}}{\Omega_1} = \frac{1}{\Omega_1} \left(\frac{du}{dr} - \frac{u}{r} \right) \\ &= \frac{2\eta_v}{1 + \eta_v} \left(\frac{N(I_0(\varepsilon\kappa) - 2I_1(\varepsilon\kappa)/\varepsilon\kappa)}{-O(K_0(\varepsilon\kappa) + 2K_1(\varepsilon\kappa)/\varepsilon\kappa)} \right) S^{-1} - \frac{2(\mu - QS^{-1})}{\kappa^2}. \end{aligned} \tag{32}$$

Now, from (16), (17), (28) and (29), the solutions (25), (26), (30)–(32) can be reduced to special cases of Couette flow. For $\eta_v = 0$, we have the expressions for u , ω , $t_{r\theta}$, $t_{\theta r}$, m_{rz} , m_{zr} and $2\dot{\gamma}$:

$$u = Cr + \frac{D}{r}, \tag{33}$$

$$\omega = E \ln r + F, \tag{34}$$

$$t_{r\theta} = t_{\theta r} = \eta \left(\frac{du}{dr} - \frac{u}{r} \right) = -\frac{2D}{r^2}\eta, \tag{35}$$

$$m_{rz} = \frac{\gamma}{\beta}m_{zr} = \gamma \frac{d\omega}{dr} = \gamma \frac{E}{r}, \tag{36}$$

$$2\dot{\gamma} = -\frac{2D}{r^2}, \tag{37}$$

where

$$\left. \begin{aligned} C &= \Omega_1(\mu - \zeta^2)/(1 - \zeta^2), \quad D = \Omega_1 R_1^2(1 - \mu)/(1 - \zeta^2), \\ E &= \Omega_1(1 - \mu)/\ln \zeta, \quad F = \Omega_1(1 - \ln R_1(1 - \mu)/\ln \zeta). \end{aligned} \right\} \tag{38}$$

Equations (33), (35) and (37) are the classical analytical solutions. The non-polar behaviour can be observed by examining the constitutive relations (8) and (9). If $\eta_R = 0$, then the shear stress will not be affected by the microrotation, and the couple

stress will not be affected by the velocity field. Thus, the vortex viscosity parameter (or microstructure parameter), in a sense, allows us to measure the deviation of flow of micropolar fluids from that of non-polar fluids. For $\eta_s = 0$, the expressions of u and $2\dot{\gamma}$ are classical ones, but those of ω , $t_{r\theta}$, $t_{\theta r}$, m_{rz} and m_{zr} become

$$\omega = C, \tag{39}$$

$$t_{r\theta} = t_{\theta r} = -2\eta \frac{D}{r^2}, \tag{40}$$

$$m_{rz} = m_{zr} = 0. \tag{41}$$

The constant value of the microrotation velocity shows that the boundary conditions are unsatisfied. Hence, in addition to additional kinematic measures must be introduced to describe internal spin, couple stresses should be present in Couette flow of fluids with microstructure.

It should be noted that Ariman *et al.* (1967), Verma & Sehgal (1968) and Sastry & Das (1985) used conventional microrotation velocity boundary conditions (zero microrotation velocity components at the wall surfaces). By using this wall-surface law, the dimensionless solutions of the velocity field, microrotation velocity field, shear stress difference, couple stress and strain rate are given by

$$U(\kappa) = \left(\frac{2\eta_v}{1 + \eta_v} \frac{1}{\zeta \varepsilon} (\mu - \zeta^2) \left(\frac{d(I_1(\varepsilon\kappa) - I_1(\varepsilon)/\kappa)}{+e(K_1(\varepsilon\kappa) - K_1(\varepsilon)/\kappa)} \right) \right) S^{-1} + \frac{\mu}{\zeta \kappa}, \tag{42}$$

$$\Omega(\kappa) = (\mu - \zeta^2) (d(I_0(\varepsilon\kappa) - I_0(\zeta\varepsilon)) - e(K_0(\varepsilon\kappa) - K_0(\zeta\varepsilon))) S^{-1}, \tag{43}$$

$$T_{r\theta}(\kappa) = 4\eta_v (\mu - \zeta^2) (dI_0(\varepsilon\kappa) - eK_0(\varepsilon\kappa)) \left(\frac{\eta_v}{1 + \eta_v} - 1 \right) S^{-1}, \tag{44}$$

$$M_{rz}(\kappa) = \zeta \varepsilon (\mu - \zeta^2) (dI_1(\varepsilon\kappa) + eK_1(\varepsilon\kappa)) S^{-1}, \tag{45}$$

$$\dot{\Gamma}(\kappa) = \frac{2\eta_v}{1 + \eta_v} (\mu - \zeta^2) \left(\frac{d \left(I_0(\varepsilon\kappa) - \frac{2}{\lambda\kappa} I_1(\varepsilon\kappa) \right)}{-e \left(K_0(\varepsilon\kappa) + \frac{2}{\lambda\kappa} K_1(\varepsilon\kappa) \right)} \right) S^{-1} - \frac{2L}{\kappa^2}, \tag{46}$$

where

$$L = \mu - (\mu - \zeta^2) \left(-dI_0(\zeta\varepsilon) + eK_0(\zeta\varepsilon) + \frac{2\eta_v}{1 + \eta_v} \frac{1}{\varepsilon} (dI_1(\varepsilon) + eK_1(\varepsilon)) \right) S^{-1}. \tag{47}$$

For $\eta_v = 0$, the solutions inconsistent with the present ones are

$$\omega = 0, \tag{48}$$

$$m_{rz} = m_{zr} = 0. \tag{49}$$

In the past, (48) and (49) were believed to be the closed form solutions in Couette flow of fluids without microstructure.

2.3. Field equations with disturbance

To study the stability of Couette flow, we superimpose a general disturbance on the basic solution in the form

$$\mathbf{u} = (u'_r, u(r) + u'_\theta, u'_z), \quad p = p(r) + p', \quad \boldsymbol{\omega} = (\omega'_r, \omega'_\theta, \omega(r) + \omega'_z), \tag{50}$$

where (u'_r, u'_θ, u'_z) , p' and $(\omega'_r, \omega'_\theta, \omega'_z)$ represent the small perturbations in the velocity, pressure and microrotation velocity, respectively. Substituting (50) into (5)–(7), and

neglecting quadratic terms in the usual way, we can obtain the resultant disturbance equations:

$$\frac{\partial u'_r}{\partial r} + \frac{u'_r}{r} + \frac{1}{r} \frac{\partial u'_\theta}{\partial \theta} + \frac{\partial u'_z}{\partial z} = 0, \quad (51)$$

$$\rho \left(\frac{\partial u'_r}{\partial t} + \frac{u}{r} \frac{\partial u'_r}{\partial \theta} - \frac{2u}{r} u'_\theta \right) = -\frac{\partial p'}{\partial r} + (\eta + \eta_R) \left(\Delta u'_r - \frac{u'_r}{r^2} - \frac{2}{r^2} \frac{\partial u'_\theta}{\partial \theta} \right) + 2\eta_R \left(\frac{1}{r} \frac{\partial \omega'_z}{\partial \theta} - \frac{\partial \omega'_\theta}{\partial z} \right), \quad (52)$$

$$\rho \left(\frac{\partial u'_\theta}{\partial t} + (D'_* u) u'_r + \frac{u}{r} \frac{\partial u'_\theta}{\partial \theta} \right) = -\frac{1}{r} \frac{\partial p'}{\partial \theta} + (\eta + \eta_R) \left(\Delta u'_\theta - \frac{u'_\theta}{r^2} + \frac{2}{r^2} \frac{\partial u'_r}{\partial \theta} \right) + 2\eta_R \left(\frac{\partial \omega'_r}{\partial z} - \frac{\partial \omega'_z}{\partial r} \right), \quad (53)$$

$$\rho \left(\frac{\partial u'_z}{\partial t} + \frac{u}{r} \frac{\partial u'_z}{\partial \theta} \right) = -\frac{\partial p'}{\partial z} + (\eta + \eta_R) \Delta u'_z + 2\eta_R \left(D'_* \omega'_\theta - \frac{1}{r} \frac{\partial \omega'_r}{\partial \theta} \right), \quad (54)$$

$$\rho \phi \left(\frac{\partial \omega'_r}{\partial t} + \frac{u}{r} \frac{\partial \omega'_r}{\partial \theta} - \frac{u \omega'_\theta}{r} \right) = (\alpha + \beta) \frac{\partial}{\partial r} \left(\frac{1}{r} \frac{\partial (r \omega'_r)}{\partial r} + \frac{1}{r} \frac{\partial \omega'_\theta}{\partial \theta} + \frac{\partial \omega'_z}{\partial z} \right) - 4\eta_R \omega'_r + 2\eta_R \left(\frac{1}{r} \frac{\partial u'_z}{\partial \theta} - \frac{\partial u'_\theta}{\partial z} \right) + \gamma \left(\Delta \omega'_r - \frac{\omega'_r}{r^2} - \frac{2}{r^2} \frac{\partial \omega'_\theta}{\partial \theta} \right), \quad (55)$$

$$\rho \phi \left(\frac{\partial \omega'_\theta}{\partial t} + \frac{u}{r} \frac{\partial \omega'_\theta}{\partial \theta} + \frac{u \omega'_r}{r} \right) = (\alpha + \beta) \frac{1}{r} \frac{\partial}{\partial \theta} \left(\frac{1}{r} \frac{\partial (r \omega'_r)}{\partial r} + \frac{1}{r} \frac{\partial \omega'_\theta}{\partial \theta} + \frac{\partial \omega'_z}{\partial z} \right) - 4\eta_R \omega'_\theta + 2\eta_R \left(\frac{\partial u'_r}{\partial z} - \frac{\partial u'_z}{\partial r} \right) + \gamma \left(\Delta \omega'_\theta - \frac{\omega'_\theta}{r^2} + \frac{2}{r^2} \frac{\partial \omega'_r}{\partial \theta} \right), \quad (56)$$

$$\rho \phi \left(\frac{\partial \omega'_z}{\partial t} + \frac{u}{r} \frac{\partial \omega'_z}{\partial \theta} + (D' \omega) u'_r \right) = (\alpha + \beta) \frac{\partial}{\partial z} \left(\frac{1}{r} \frac{\partial (r \omega'_r)}{\partial r} + \frac{1}{r} \frac{\partial \omega'_\theta}{\partial \theta} + \frac{\partial \omega'_z}{\partial z} \right) - 4\eta_R \omega'_z + \frac{2\eta_R}{r} \left(\frac{\partial (r u'_\theta)}{\partial r} - \frac{\partial u'_r}{\partial \theta} \right) + \gamma \Delta \omega'_z, \quad (57)$$

where

$$\Delta = \frac{\partial^2}{\partial r^2} + \frac{1}{r} \frac{\partial}{\partial r} + \frac{1}{r^2} \frac{\partial^2}{\partial \theta^2} + \frac{\partial^2}{\partial z^2}. \quad (58)$$

The boundary conditions on velocity and microrotation velocity are

$$u'_r = u'_\theta = u'_z = \omega'_r = \omega'_\theta = \omega'_z = 0 \quad \text{at} \quad r = R_1 \quad \text{and} \quad r = R_2. \quad (59)$$

2.4. Eigenvalue problem

The linearized problem for the stability of Couette flow can lead to a simplified eigenvalue problem by making a normal mode analysis. Since the coefficients in the resultant equations depend only on r , it is possible to look for solutions of the form:

$$\left. \begin{aligned} (u'_r, u'_\theta, u'_z) &= \bar{d} \Omega_1(u'(x), v'(x), w'(x)) e^{i(st+m\theta+\lambda z)}, \\ p' &= \eta \Omega_1 \pi'(x) e^{i(st+m\theta+\lambda z)}, \\ (\omega'_r, \omega'_\theta, \omega'_z) &= \Omega_1(e'(x), f'(x), g'(x)) e^{i(st+m\theta+\lambda z)}, \end{aligned} \right\} \quad (60)$$

where (u', v', w') , π' and (e', f', g') are the varying quantities of the small disturbance velocity, pressure and microrotation velocity, respectively, and x is the ratio $(r - R_1)/\bar{d}$. It is assumed that s is a complex number, λ is a real number and m is an integer. Without loss of generality, we can take m to be zero or a positive integer.

We now introduce the following dimensionless variables:

$$\left. \begin{aligned} \xi(x) &= \bar{d}/(R_1 + x\bar{d}), \quad \psi = \rho\Omega_1\phi/\eta, \quad a = \bar{d}\lambda, \\ \sigma &= \rho s \bar{d}^2/\eta, \quad T = -4\Omega_1^2 \bar{d}^4 \rho^2 (\mu - \zeta^2)/\eta^2 (1 - \zeta^2), \end{aligned} \right\} \quad (61)$$

where T represents the Taylor number. Substituting (60) and (61) into the linearized disturbance equations, we obtain the following system of ordinary differential equations:

$$\left. \begin{aligned} D_* u' &= -im\xi(x)v' - iaw', \quad D_* v' = Y, \quad Dw' = Z, \\ DX &= \bar{M}(x)u' + 2 \left(im\xi^2(x) - \sqrt{T}\bar{\Omega}^*(x) \right) v' - 2im\eta_v \xi(x)g' + 2ia\eta_v f' \\ &\quad + im\eta_v \xi(x)Y + ia\eta_v Z, \\ (1 + \eta_v)DY &= -(2im(1 + \eta_v)\xi^2(x) - \sqrt{T}\bar{\Omega}^*(x))u' + (\bar{M}(x) + m^2\xi^2(x))v' \\ &\quad + am\xi(x)w' - 2ia\eta_v e' - im\xi(x)X + 2\eta_v \bar{Z}, \\ (1 + \eta_v)D_* Z &= am\xi(x)v' + (\bar{M}(x) + a^2)w' + 2im\eta_v \xi(x)e' - iaX - 2\eta_v \bar{Y}, \\ D_* e' &= \bar{X}, \quad D_* f' = \bar{Y}, \quad Dg' = \bar{Z}, \\ (\eta_s + \eta_b)D\bar{X} &= 2ia\eta_v v' - 2im\eta_v \xi(x)w' + (4\eta_v + m^2\eta_s \xi^2(x) + a^2\eta_s)e' \\ &\quad + 2(im(\eta_s + \eta_b)\xi^2(x))f' - im\eta_b \xi(x)\bar{Y} - ia\eta_b \bar{Z} \\ &\quad + i\psi \hat{M}(x)e' - \psi \hat{\Omega}^*(x)f', \\ \eta_s D\bar{Y} &= -2ia\eta_v u' - 2im\eta_s \xi^2(x)e' + (4\eta_v + m^2\eta_s \xi^2(x) + a^2\eta_s + m^2\eta_b \xi^2(x))f' \\ &\quad + ma\eta_b \xi(x)g' - im\eta_b \xi(x)\bar{X} + 2\eta_v Z \\ &\quad + i\psi \hat{M}(x)f' + \psi \hat{\Omega}^*(x)e', \\ \eta_s D_* \bar{Z} &= 2im\eta_v \xi(x)e' + ma\eta_b \xi(x)f' + (4\eta_v + m^2\eta_s \xi^2(x) + a^2(\eta_s + \eta_b))g' \\ &\quad - ia\eta_b \bar{X} - 2\eta_v \bar{Y} \\ &\quad + i\psi \hat{M}(x)g' + \psi \hat{\Omega}^*(x)u', \end{aligned} \right\} \quad (62)$$

where

$$\left. \begin{aligned} D &= \frac{d}{dx}, \quad D_* = \frac{d}{dx} + \xi(x), \quad \hat{A} = \frac{A}{\Omega_1}, \quad \hat{B} = \frac{B}{\Omega_1}, \quad \hat{C} = \frac{C}{\Omega_1}, \quad \hat{D} = \frac{\xi^2(x)D}{\Omega_1 R_2^2 (1 - \zeta)^2}, \\ \bar{A} &= \frac{1}{2} \left(-\frac{\Omega_1^2 (\mu - \zeta^2)}{1 - \zeta^2} \right)^{-1/2} \frac{2\eta_v}{1 + \eta_v} A, \quad \bar{B} = -\frac{1}{2} \left(-\frac{\Omega_1^2 (\mu - \zeta^2)}{1 - \zeta^2} \right)^{-1/2} \frac{2\eta_v}{1 + \eta_v} B, \\ \bar{C} &= \frac{1}{2} \left(-\frac{\Omega_1^2 (\mu - \zeta^2)}{1 - \zeta^2} \right)^{-1/2} C, \quad \bar{d} = \frac{1}{2} \left(-\frac{\Omega_1^2 (\mu - \zeta^2)}{1 - \zeta^2} \right)^{-1/2} \frac{1}{\bar{d}^2} D, \\ \hat{M}(x) &= 2\sigma \left(-\frac{T(1 - \zeta^2)}{\mu - \zeta^2} \right)^{-1/2} + m\hat{\Omega}^*(x), \\ \bar{M}(x) &= (1 + \eta_v)(a^2 + m^2\xi^2(x)) + i \left(\sigma + m\sqrt{T}\bar{\Omega}^*(x) \right), \\ \hat{\Omega}^*(x) &= \frac{2\eta_v}{1 + \eta_v} \frac{\xi(x)}{k\bar{d}} \left(\hat{A}I_1 \left(\frac{k\bar{d}}{\xi(x)} \right) - \hat{B}K_1 \left(\frac{k\bar{d}}{\xi(x)} \right) \right) + \hat{C} + \hat{D}, \\ \bar{\Omega}^*(x) &= \bar{A} \frac{\xi(x)}{k\bar{d}} I_1 \left(\frac{k\bar{d}}{\xi(x)} \right) + \bar{B} \frac{\xi(x)}{k\bar{d}} K_1 \left(\frac{k\bar{d}}{\xi(x)} \right) + \bar{C} + \bar{D}\xi^2(x), \\ \hat{\Omega}^*(x) &= k\bar{d}\hat{A}I_1 \left(\frac{k\bar{d}}{\xi(x)} \right) - k\bar{d}\hat{B}K_1 \left(\frac{k\bar{d}}{\xi(x)} \right) \\ \bar{\Omega}^*(x) &= \bar{A}I_0 \left(\frac{k\bar{d}}{\xi(x)} \right) - \bar{B}K_0 \left(\frac{k\bar{d}}{\xi(x)} \right) + 2\bar{C}. \end{aligned} \right\} \quad (63)$$

The boundary conditions at $x = 0$ and $x = 1$ are

$$u' = v' = w' = e' = f' = g' = 0. \tag{64}$$

The set of equations (62) with the boundary conditions (64) determines an eigenvalue problem in the form:

$$F(\eta_v, \eta_s, \eta_b, \psi, \mu, \zeta, a, m, \sigma, T) = 0. \tag{65}$$

The marginal state is characterized by the imaginary part of σ , σ_i , equal to zero. For given values of $\eta_v, \eta_s, \eta_b, \psi, \mu$ and ζ , we seek the minimum positive real value of T for all positive real numbers a and non-negative integers m , for which there is a solution of (65) with $\sigma_i = 0$. This value of T sought is the critical Taylor number T_c . The values of a and m corresponding to T_c determine the onset mode of instability. Moreover, the real part of σ , σ_r corresponding to T_c determines the frequency of oscillation. The critical disturbance is called the axisymmetric stationary mode if $m = 0$ and $\sigma_r = 0$, the axisymmetric oscillation mode if $m = 0$ and $\sigma_r \neq 0$, and the non-axisymmetric mode if $m \neq 0$. For a fixed value of z , the wave will propagate in the direction of the basic flow with an angular velocity (in units of Ω_1) given by $c = -\eta\sigma_r / \rho md^2 \Omega_1$. We solve the two-point eigenvalue problem defined by (62) and (64) by a shooting technique. The details of the procedure are discussed below.

A set of six linearly independent solutions of the system of differential equations (62) which satisfy the boundary condition at $x = 0$ can be constructed by imposing the initial conditions:

$$(u'_j, v'_j, w'_j, e'_j, f'_j, g'_j, X_j, Y_j, Z_j, \bar{X}_j, \bar{Y}_j, \bar{Z}_j) = \left. \begin{array}{l} \left(\begin{array}{cccccccccccc} 0 & 0 & 0 & 0 & 0 & 0 & 1 & 0 & 0 & 0 & 0 & 0 \end{array} \text{ for } j = 1, \\ \left(\begin{array}{cccccccccccc} 0 & 0 & 0 & 0 & 0 & 0 & 0 & 1 & 0 & 0 & 0 & 0 \end{array} \text{ for } j = 2, \\ \left(\begin{array}{cccccccccccc} 0 & 0 & 0 & 0 & 0 & 0 & 0 & 0 & 1 & 0 & 0 & 0 \end{array} \text{ for } j = 3, \\ \left(\begin{array}{cccccccccccc} 0 & 0 & 0 & 0 & 0 & 0 & 0 & 0 & 0 & 1 & 0 & 0 \end{array} \text{ for } j = 4, \\ \left(\begin{array}{cccccccccccc} 0 & 0 & 0 & 0 & 0 & 0 & 0 & 0 & 0 & 0 & 1 & 0 \end{array} \text{ for } j = 5, \\ \left(\begin{array}{cccccccccccc} 0 & 0 & 0 & 0 & 0 & 0 & 0 & 0 & 0 & 0 & 0 & 1 \end{array} \text{ for } j = 6, \end{array} \right\} \text{ as } x = 0. \tag{66}$$

Any solution of the system of (62) satisfying the boundary condition at $x = 0$ can be represented as a linear combination of these solutions. A necessary condition that this linear combination also satisfies the boundary condition $u' = v' = w' = e' = f' = g' = 0$ at $x = 1$ is the vanishing of the determinant

$$F(\eta_v, \eta_s, \eta_b, \psi, \mu, \zeta, a, m, \sigma, T) \equiv \begin{vmatrix} u'_j \\ v'_j \\ w'_j \\ e'_j \\ f'_j \\ g'_j \end{vmatrix} = 0 \quad \text{for } j = 1 \sim 6, \quad \text{as } x = 1. \tag{67}$$

This is the required characteristic equation, from which the curve of neutral stability can be obtained. Here, we choose three pairs of trial points in the plane (T, σ_r) to determine a root of these equations for fixed values of $\eta_v, \eta_s, \eta_b, \psi, \mu, \zeta, a$ and m . For each pair of trial points, the set of solutions was obtained by using the Runge-Kutta method to solve the system of first-order equations (62). The bivariate interpolation was then used to obtain an approximation to the root. Once

η_v	η_s	η_b	ψ	ζ	μ	m			a_c			T_c			
						[A1]	[A2]	[B]	[A1]	[A2]	[B]	[A1]	[A2]	[B]	
0	0	0	0	0.95	0	0	0	0	3.132	3.132	3.128	3510	3510	3510	
					-1	4	4	4	3.685	3.686	3.680	20068	20068	20072	
					-1.25	5	5	5	3.777	3.776	3.774	30619	30619	30632	
					0.95	4	4	4	3.685	3.686	3.680	20068	20067	20072	
					0.9	-1	3	3	3	3.728	3.727	3.721	23855	23855	23861
					0.8	-1	2	2	2	3.840	3.839	3.835	36751	36751	36767
1/3	1/3	1/15	0	0.95	0.87	0	0	0	3.125	3.126	3.117	2898	3058	3023	
					0.66	0	0	0	3.126	3.126	3.117	3435	3461	3400	
					0.41	0	0	0	3.127	3.127	3.117	4082	4101	4020	
					0.17	0	0	0	3.130	3.130	3.121	4956	4980	4797	
					0	0	0	0	3.136	3.136	3.125	5830	5863	5615	
						[A1]	[A2]	[C]	[A1]	[A2]	[C]	[A1]	[A2]	[C]	

TABLE 1. Comparison of the results of the present study ([A1] and [A2]) with those of Krueger *et al.* (1966) ([B]) and Sastry & Das (1985) ([C]). [A1] denotes the case with no-slip conditions, and [A2] denotes the case with slip conditions.

the sufficiently accurate root was determined, the process was repeated for a sufficient number of values of a , so that the minimum of T for a fixed value of m , T_c^m , could be determined by using the quadratic polynomial interpolation with an interval in a of 0.2. Finally, the entire process was repeated for other values of m , so that the minimum of T_c^m , T_c and the corresponding values of a , σ_r and c could be obtained for the assigned values of η_v , η_s , η_b , ψ , μ and ζ .

3. Results and discussion

We pay attention to the influence of non-zero wall-surface microrotation velocity on the basic flow and the onset of instability for a kerosene-based suspension, in which fine iron powder is dispersed. At room temperature ($K = 298.15$ K), the density of carrier liquid is $\rho_0 = 8.17 \times 10^2 \text{ kg m}^{-3}$, the density of powder is $\rho_s = 5.24 \times 10^3 \text{ kg m}^{-3}$ and the shear viscosity of carrier liquid is $\eta_0 = 1.38 \times 10^{-3} \text{ kg m}^{-1} \text{ s}^{-1}$. The fluid density can be obtained by $\rho = \rho_s \varphi + \rho_0(1 - \varphi)$. Recall that a micropolar fluid model is better used to represent rheological behaviour for flow simulations at the small scale. The gap size of the annulus \bar{d} is set to 0.1 mm. It should be noted that the molecular structure of carrier liquid may play an important role in the space with dimensions down to the micrometre scale (Papautsky 1999).

First, we validate the code by comparing our numerical results with those of Krueger *et al.* (1966) and Sastry & Das (1985). Since the work of Krueger *et al.* is only a special case of the present study when microstructure, couple stresses and microinertia are absent, we conduct calculations for $\eta_v = \eta_s = \eta_b = \psi = 0$ and check our results in terms of T_c , a_c and m for both of the no-slip-boundary case ([A1] – non-zero microrotation velocity components at the wall surfaces) and the slip-boundary case ([A2] – zero components) with the corresponding data obtained by them. Here, $\eta_v = \eta_s = \eta_b = \psi = 0$ means that the values of η_v , η_s , η_b and ψ are much less than 10^{-6} . The comparison is in excellent agreement and the percentage difference based on T_c is generally less than 0.044 % as shown in table 1. Another check is made by considering the slip-boundary case of a micropolar fluid ($\eta_v = 1/3$, $\eta_s = 1/3$, $\eta_b = 1/15$, and $\psi = 0$: $\varphi = 2.22 \times 10^{-1}$, $\rho = 1.80 \times 10^3 \text{ kg m}^{-3}$, $\eta = 2.15 \times 10^{-3} \text{ kg m}^{-1} \text{ s}^{-1}$, $\gamma = 7.16 \times$

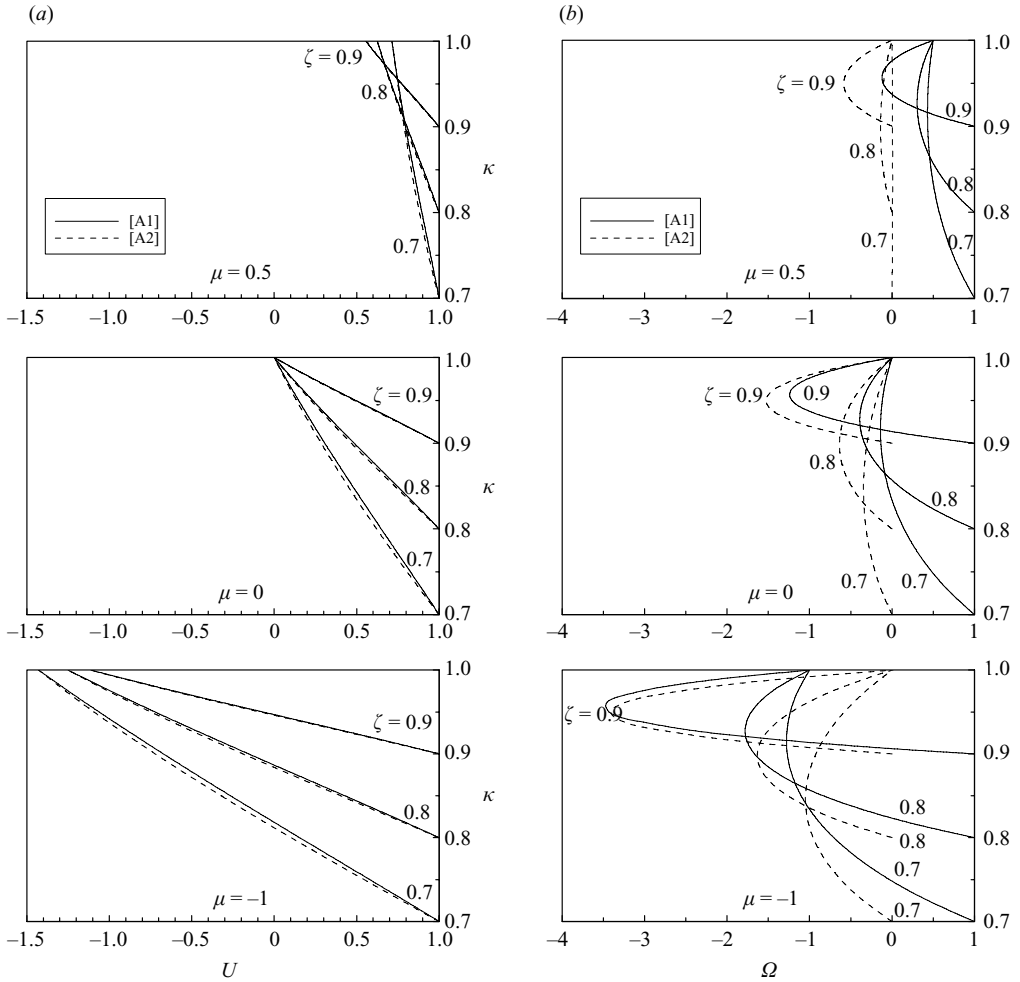


FIGURE 1. (a) Velocity distribution, (b) microrotation velocity distribution for three typical values of μ at different values of ζ with $\eta_v = 0.4$, $\eta_s = 0.4$, $\eta_b = 0.1$ and $\psi = 1$. [A1] denotes the case with no-slip conditions, and [A2] denotes the case with slip conditions.

$10^{-12} \text{ kg m s}^{-1}$ and $\alpha + \beta = 1.43 \times 10^{-12} \text{ kg m s}^{-1}$) carried out by Sastry & Das. The agreement is still quite good and the differences in T_c are less than 4.23%. Note that the results of Sastry & Das were obtained under the assumption of small-gap approximation ($\zeta \rightarrow 1$) which causes more apparent disagreement.

From table 1, it seems that the effect of non-zero wall-surface microrotation velocity on the small-gap Couette flow of a specific fluid is negligible. To extend the analysis, calculations have been performed over wide ranges of the microstructure parameter ($0 \leq \eta_v \leq 0.5 : 0 \leq \varphi \leq 3.33 \times 10^{-1}$), the couple-stress parameter ($0 \leq \eta_s \leq 1 : 0 \leq \gamma \leq 2.53 \times 10^{-11} \text{ kg m s}^{-1}$) the microinertia parameter ($0 \leq \psi \leq 10$), the radius ratio ($0.7 \leq \zeta \leq 0.95$) and the angular velocity ratio ($-1.5 \leq \mu \leq 0.9$). Note that the negligible effect of bulk spin viscosity, characterized by η_b , has been validated by calculations. The value of η_b chosen for the analysis is 0.1 ($\alpha + \beta = 2.53 \times 10^{-12} \text{ kg m s}^{-1}$).

For simplicity, now we pay attention to two flow fields: the velocity U and the microrotation velocity Ω . Figure 1(a) illustrates the variations of U with the position

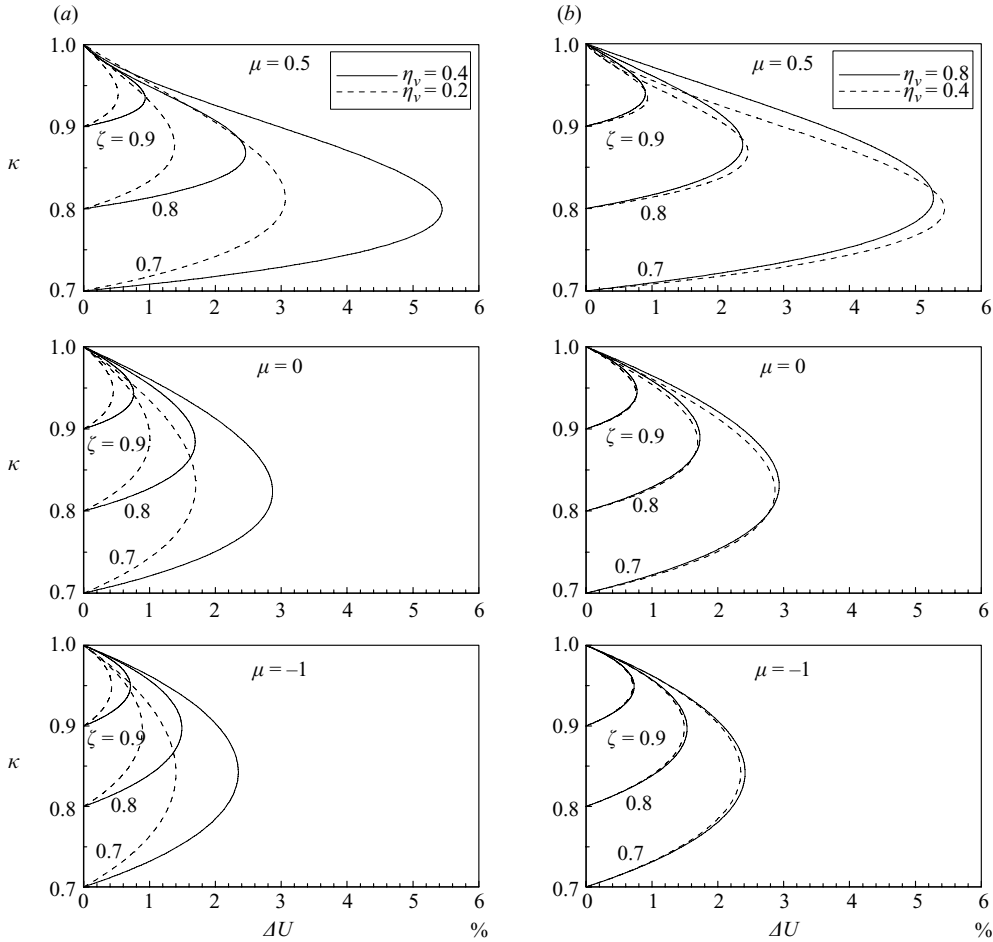


FIGURE 2. Influence of the (a) microstructure parameter η_v , (b) couple-stress parameter η_s on the normalized velocity difference between the no-slip-boundary case ([A1]) and the slip-boundary case ([A2]). The solid line denotes the solution obtained at a higher value of the parameter, and the dashed line denotes the solution obtained at a lower value.

parameter κ for three typical values of μ . The corresponding variations of Ω are shown in figure 1(b). Results reveal that the improvement in wall-surface microrotation velocity results in additional quantity in U and apparent disagreement in Ω . This effect is magnified by decreasing the radius ratio ζ .

In figure 2, we plot the normalized difference between the no-slip-boundary velocity $U_{[A1]}$ and the slip-boundary velocity $U_{[A2]}$,

$$\Delta U = \frac{U_{[A1]} - U_{[A2]}}{U(\zeta) - U(1)}, \tag{68}$$

for three typical values of μ at different values of ζ obtained under both the higher and lower value parameters of η_v and η_s . The reference values of η_s and η_v in figures 2(a) and 2(b) are 0.4. It is found from figure 2(a) that for most situations, the increase of the microstructure parameter η_v leads to an enhancement of the difference. The microstructure effect increases with increasing μ and decreasing ζ . From figure 2(b),

ζ	μ	m		a_c		T_c		σ_r		c	
		[A1]	[A2]	[A1]	[A2]	[A1]	[A2]	[A1]	[A2]	[A1]	[A2]
0.9	0.8	0	0	3.129	3.132	2543	3522	0	0	0	0
	0.6	0	0	3.127	3.127	3891	3964	0	0	0	0
	0.4	0	0	3.127	3.128	4525	4578	0	0	0	0
	0.2	0	0	3.129	3.130	5359	5420	0	0	0	0
	0	0	0	3.135	3.136	6544	6635	0	0	0	0
	-0.2	0	0	3.149	3.151	8361	8520	0	0	0	0
	-0.4	0	0	3.186	3.193	11 436	11 761	0	0	0	0
	-0.6	0	0	3.317	3.340	17 318	18 078	0	0	0	0
	-0.689	0	1	3.449	3.487	21 618	22 729	0	-9.634	0	0.3559
	-0.704	1	1	3.477	3.513	22 478	23 605	-9.572	-9.860	0.3572	0.3594
0.8	-0.8	2	2	3.584	3.611	27 963	29 333	-20.991	-21.729	0.3623	0.3667
	-1	3	3	3.678	3.694	40 923	42 985	-35.593	-36.523	0.3583	0.3588
	0.6	0	0	3.128	3.132	3535	4077	0	0	0	0
	0.4	0	0	3.128	3.131	4628	4768	0	0	0	0
	0.2	0	0	3.131	3.133	5622	5762	0	0	0	0
	0	0	0	3.137	3.141	7060	7274	0	0	0	0
	-0.2	0	0	3.154	3.162	9393	9807	0	0	0	0
	-0.4	0	0	3.211	3.234	13 736	14 712	0	0	0	0
	-0.6	0	0	3.445	3.536	23 105	25 729	0	0	0	0
	-0.605	0	1	3.456	3.533	23 448	26 123	0	-15.039	0	0.3433
0.7	-0.634	1	1	3.512	3.580	25 562	28 310	-14.842	-15.777	0.3464	0.3503
	-0.8	2	2	3.667	3.705	38 149	42 118	-33.929	-35.683	0.3441	0.3445
	-1	2	2	3.730	3.779	58 658	66 119	-41.821	-44.757	0.3653	0.3684
	0.4	0	0	3.128	3.136	4631	5005	0	0	0	0
	0.2	0	0	3.132	3.138	5956	6200	0	0	0	0
	0	0	0	3.139	3.147	7759	8146	0	0	0	0
	-0.2	0	0	3.162	3.178	10 909	11 768	0	0	0	0
	-0.4	0	0	3.260	3.322	17 590	20 088	0	0	0	0
	-0.524	0	1	3.470	3.588	26 079	31 124	0	-20.592	0	0.3266
	-0.565	1	1	3.553	3.648	30 065	35 322	-20.136	-22.135	0.3313	0.3363
0.7	-0.6	1	1	3.601	3.718	33 296	39 361	-21.443	-23.654	0.3413	0.3472
	-0.8	2	2	3.821	3.892	57 011	67 035	-48.513	-52.447	0.3191	0.3183
	-1	2	2	3.849	3.911	88 550	107 159	-58.794	-65.268	0.3331	0.3363

TABLE 2. Critical parameters for various values of μ at three assigned values of ζ with $\eta_v = 0.4$, $\eta_s = 0.4$, $\eta_b = 0.1$, and $\psi = 1$. [A1] denotes the case with no-slip conditions, and [A2] denotes the case with slip conditions.

the couple-stress effect is found to shift the asymmetric profile of ΔU to the outer-cylinder side. This effect also increases with increasing μ and decreasing ζ .

The variations of Re_{1c} , a_c , σ_r and c as a function of the Re_2 for the no-slip-boundary case ([A1]) and the slip-boundary case ([A2]) at different values of ζ with $\eta_v = 0.4$, $\eta_s = 0.4$, $\eta_b = 0.1$ and $\psi = 1$ are shown in figure. The specific data are given in table 2, and the specific neutral curves are illustrated in figure 4. Note that the critical inner-cylinder Reynolds number Re_{1c} and the outer-cylinder Reynolds number Re_2 are defined as

$$Re_{1c} = \frac{\rho R_1 \Omega_1 \bar{d}}{\eta} = \frac{1}{2(1/\zeta - 1)} \sqrt{\frac{1 - \zeta^2}{\zeta^2 - \mu}} T_c, \tag{69}$$

$$Re_2 = \frac{\rho R_2 \Omega_2 \bar{d}}{\eta} = \frac{\mu}{\zeta} Re_{1c}. \tag{70}$$

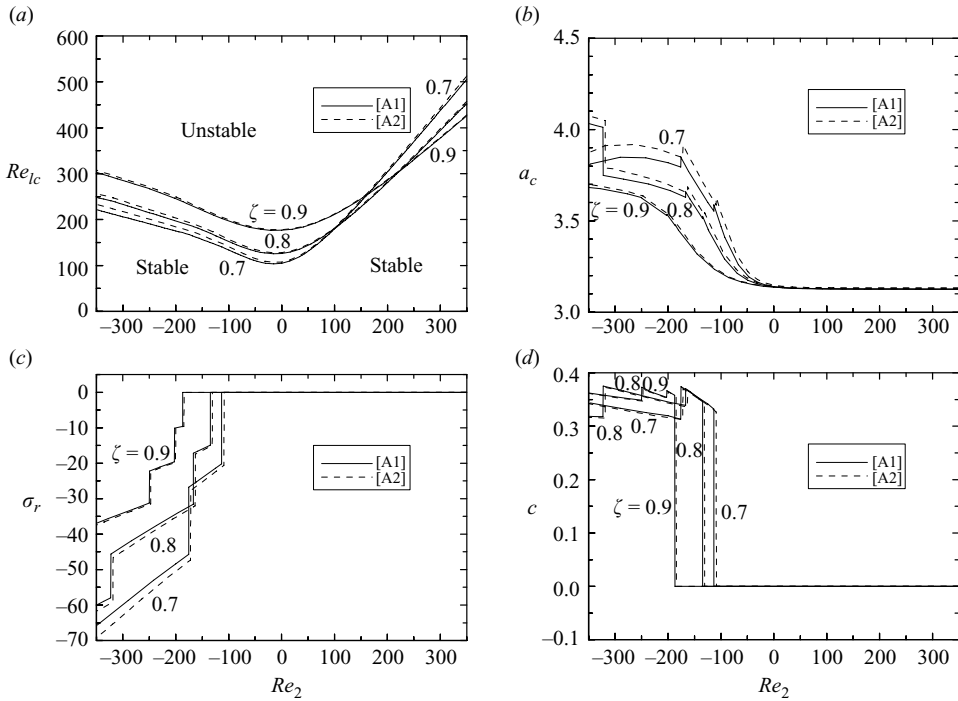


FIGURE 3. (a)–(d) Variation of Re_{1c} , a_c , σ_r and c with Re_2 at different values of ζ with $\eta_v = 0.4$, $\eta_s = 0.4$, $\eta_b = 0.1$ and $\psi = 1$. [A1] denotes the case with no-slip conditions, and [A2] denotes the case with slip conditions.

In the plane (Re_{1c}, Re_2) , the locus determined from T_c divides the plane into stable and unstable regions. It is obvious from figure 3(a) that the locus of [A1] is always below that of [A2], i.e. the no-slip-boundary case is more unstable than the slip-boundary case. The difference between the two loci is obvious especially for small values of Re_2 and ζ . The more unstable region results from the additional translational motion induced by the no-slip boundaries. In addition, table 2 shows that the critical disturbance is a non-axisymmetric mode ($m \neq 0$) as the value of μ (or Re_2) is sufficiently negative. The improvement in wall-surface microrotation velocity leads to the reduction of the limit of the critical non-axisymmetric disturbance. Figure 4 illustrates the transition processes from axisymmetric to non-axisymmetric onset modes through the neutral curves in the plane (Re_{1c}, a) . We may recall that the critical Reynolds number Re_{1c} and axial wavenumber a_c are determined by the minimum of these neutral curves. As Re_2 decrease, the curve $m = 0$ shifts up (and to the right) more quickly than the curve $m = 1$, and Re_{1c} and a_c are eventually determined by the minimum of $m = 1$. Since the minimum of the curve $m = 0$ is always located at the right-hand side of that of the curve $m = 1$, a change of onset mode may cause a sharp decrease in a_c . In figures 3(b), it shows that a sharp variation due to a change of onset mode (from m to $m \pm 1$) predicts a discontinuity of the curve. a_c increases as Re_2 decreases, except for onset mode changing or sufficiently negative values of Re_2 . The improvement in wall-surface microrotation velocity tends to reduce the values of a_c . Thus, the axial wavelength $2\pi d/a_c$ increases. In figures 3(c) and 3(d) the discontinuities of curves are also due to a change of onset mode. As the instability sets in as a non-axisymmetric mode, the oscillatory frequency σ_r decreases

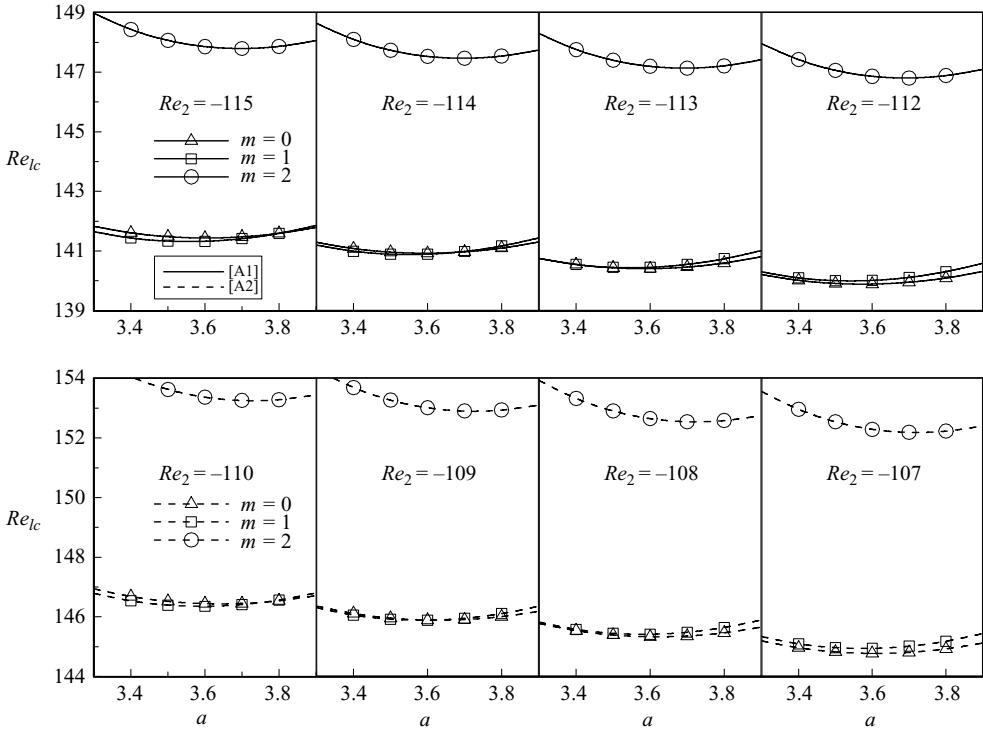


FIGURE 4. Neutral curves of different modes for four assigned values of Re_2 with $\zeta = 0.7$. [A1] denotes the case with no-slip conditions, and [A2] denotes the case with slip conditions.

with decreasing Re_2 while the angular velocity c increases. The microrotation velocity no-slip conditions generally raise the magnitudes of σ_r and c . The effect of wall-surface microrotation velocity on the stability characteristics are shown to be magnified by decreasing Re_2 and ζ .

In figure 5, we plot the microstructure and couple-stress effects on the onset of instability and the onset mode at different values of ζ with $\eta_b = 0.1$, $\psi = 1$, and $Re_2 = -170$. The reference values of η_s and η_v in figures 5(a) and 5(b) are 0.4. It is obvious that Re_{1c} increases gradually with increasing η_v and η_s , but m may decrease. This means that both microstructure and couple stresses in fluids have a stabilizing effect which may lead to onset mode changing. The data show that as the wall-surface microrotation velocity is improved, the stabilizing effect is less obvious; moreover, the limits of critical non-axisymmetric disturbances are reduced. The effect of wall-surface microrotation velocity can be magnified by increasing η_v and η_s .

Finally, to understand the role of microinertia on stability, we further plot in figure 6 the effect of microinertia (increasing ψ) on the onset of instability at different values of ζ with $Re_2 = 170$ (a case of $\mu > 0$), $Re_2 = 0$ (the case of $\mu = 0$) and $Re_2 = -170$ (a case of $\mu < 0$). It should be noted from calculations that microinertia tends to reduce the limits of critical non-axisymmetric disturbances; however, its role on the onset mode is negligible. Hence, the negligible effect is not shown here. In general, the microinertia effect is to slightly destabilize the flow, due to the contribution to the translational motion of fluid particles; however, as the radius ratio ζ decreases, it may be to slightly stabilize the flow. For instance, in the counter-rotating and no-slip-boundary case ($\mu < 0$ and [A1]), shown in figure 6, the values of Re_{1c} for

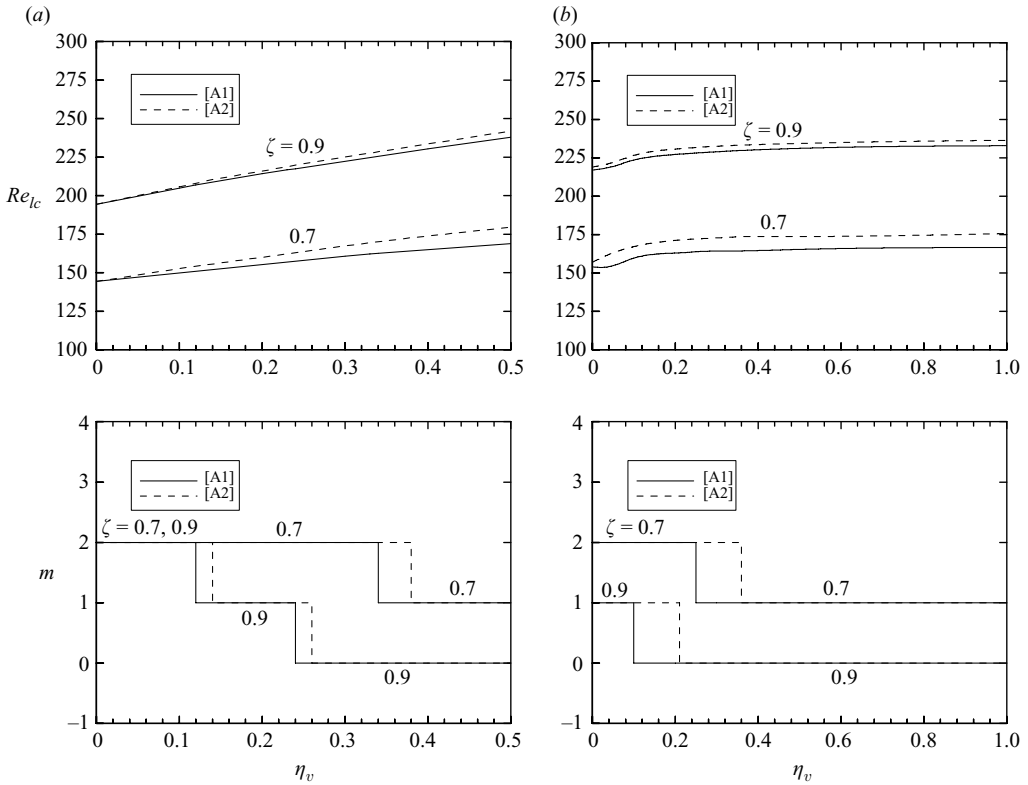


FIGURE 5. Influence of the (a) microstructure parameter η_v , (b) couple-stress parameter η_s on the critical inner-cylinder Reynolds number and the azimuthal wavenumber. The case of counter-rotating cylinders considered here is $Re_2 = -170$. [A1] denotes the case with no-slip conditions, and [A2] denotes the case with slip conditions.

$\psi = 0, 5,$ and 10 are $230.34, 229.64$ and 229.05 , respectively, at $\zeta = 0.9$ and $164.99, 165.02$ and 165.07 , respectively, at $\zeta = 0.7$. The stabilizing effect (the increase in Re_{ic} with increasing ψ) may result from the greater linear-momentum loss via particle rotation. As for the effect of wall-surface microrotation velocity, characterized here by the normalized difference between the no-slip-boundary Reynolds number and the slip-boundary Reynolds number ΔRe results show that this effect can be magnified by decreasing ψ for the case of $\mu < 0$ or by increasing the ψ for the cases of $\mu > 0$ and $\mu = 0$.

4. Conclusions

A complete analysis for the linear stability of micropolar fluid flow between two concentric rotating cylinders has been conducted. The effect of non-zero wall-surface microrotation velocity on the flow and stability characteristics with respect to the microstructure, couple-stress and microinertia parameters, and the radius and angular velocity ratios were discussed in details. Results revealed that non-zero wall-surface microrotation velocity tends to enhance the flow and to advance the onset of instability. Moreover, it was found that the same effect as microstructure, couple stresses and microinertia is to reduce the limits of critical non-axisymmetric disturbances. By increasing the effect of curvature, microstructure, or couple stresses

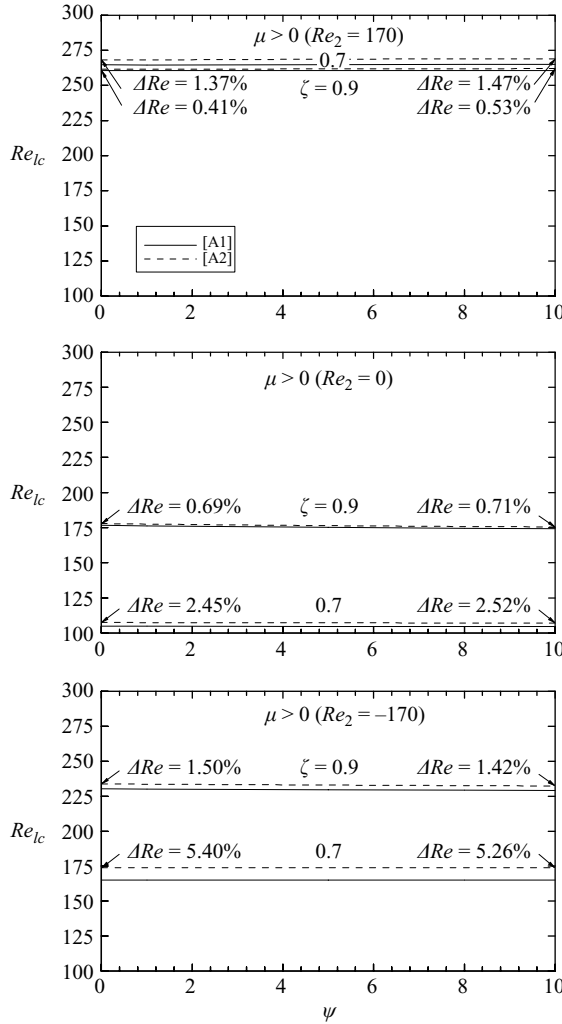


FIGURE 6. Influence of the microinertia parameter ψ on the critical inner-cylinder Reynolds number. ΔRe denotes the normalized difference between the no-slip-boundary value and the slip-boundary value, [A1] denotes the case with no-slip conditions, and [A2] denotes the case with slip conditions.

or the effect of microinertia in the cases of corotating cylinders and a stationary outer cylinder or by decreasing the effect of microinertia in the case of counterrotating cylinders, the role of non-zero wall-surface microrotation velocity on stability can be more visible. Such a type of study helps the understanding of the flow and stability problems for fluids with microstructure.

This research was supported by the National Science Council of Taiwan under grant NSC 95-2221-E-006-248 and the project of the specific research fields in the Chung Yuan Christian University, Taiwan under grant CYCU-97-CR-ME. The authors would like to thank the referees of this paper for their very helpful comments.

REFERENCES

- ALLEN, S. & KLINE, K. 1971 Lubrication theory for micropolar fluids. *J. Appl. Mech.* **38**, 64–650.
- AMBACHER, O., ODENBACH, S. & STIERSTADT, K. 1992 Rotational viscosity in ferrofluids. *Z. Phys. B: Condens. Matter* **86**, 29–32.
- ANDERECK, C. D., LIN, S. S. & SWINNEY, H. L. 1986 Flow regimes in a circular Couette system with independently rotating cylinders. *J. Fluid Mech.* **164**, 15–183.
- ARIMAN, T., CAKMAK, A. S. & HILL, L. R. 1967 Flow of micropolar fluids between two concentric cylinders. *Phys. Fluids* **10**, 2545–2550.
- ARIMAN, T., TURK, M. A. & SYLVESTER, N. D. 1973 Microcontinuum fluid mechanics – a review. *Intl J. Engng Sci.* **11**, 905–930.
- ARIMAN, T., TURK, M. A. & SYLVESTER, N. D. 1974 Applications of microcontinuum fluid mechanics. *Intl J. Engng Sci.* **12**, 273–293.
- BRENNER, H. 1970 Rheology of two-phase system. *Annu. Rev. Fluid Mech.* **2**, 137–176.
- BRUTYAN, M. A. & KRAPIVSKY, P. L. 1992 On the stability of periodic unidirectional flows of micropolar fluid. *Intl J. Engng Sci.* **30**, 40–407.
- CHANG, M. H., CHEN, C. K. & WENG, H. C. 2003 Stability of ferrofluid flow between concentric rotating cylinders with an axial magnetic field. *Intl J. Engng Sci.* **41**, 103–121.
- CHEN, C. K. & CHANG, M. H. 1998 Stability of hydromagnetic dissipative Couette flow with non-axisymmetric disturbance. *J. Fluid Mech.* **366**, 135–158.
- DAS, S., GUHA, S. K. & CHATTOPADHYAY, A. K. 2005 Linear stability analysis of hydrodynamic journal bearings under micropolar lubrication. *Tribol. Intl* **38**, 500–507.
- EINSTEIN, A. 1906 Eine neue Bestimmung der Molekuldimensionen. *Ann. Phys.* **19**, 289–306.
- EMBS J. P., MÜLLER, H. W., WAGNER, C., KNORR, K. & LÜCKE, M. 2000 Measuring the rotational viscosity of ferrofluids without shear flow. *Phys. Rev. E* **61**, R2196–R2199.
- ERINGEN, A. C. 1964 Simple microfluids. *Intl J. Engng Sci.* **2**, 205–217.
- ERINGEN, A. C. 1966 Theory of micropolar fluids. *J. Math. Mech.* **16**, 1–16.
- ERINGEN, A. C. 1993 Assessment of director and micropolar theories of liquid crystals. *Intl J. Engng Sci.* **31**, 605–616.
- ERINGEN, A. C. 2001 *Microcontinuum field theories. II: Fluent media*. Springer.
- HADIMOTO, B. & TOKIOKA, T. 1969 Two-dimensional shear flows of linear micropolar fluids. *Intl J. Engng Sci.* **7**, 515–522.
- HOLDERIED, M., SCHWAB, L. & STIERSTADT, K. 1988 Rotational viscosity of ferrofluids and the Taylor instability in a magnetic field. *Z. Phys. B: Condens. Matter* **70**, 431–433.
- KANG, C. K. & ERINGEN, A. C. 1976 The effect of microstructure on the rheological properties of blood. *Bull. Math. Biol.* **38**, 135–159.
- KHONSARI, M. M. 1990 On the self-excited whirl orbits of a journal in a Sleeve bearing lubricated with micropolar fluids. *Acta Mech.* **81**, 235–244.
- KHONSARI, M. M. & BREWE, D. E. 1989 On the performance of finite journal bearings lubricated with micropolar fluids. *STLE Tribol. Trans.* **32**, 15–160.
- KRUEGER, E. R., GROSS, A. & DIPRIMA, R. C. 1966 On the relative importance of Taylor-vortex and non-axisymmetric modes in flow between rotating cylinders, *J. Fluid Mech.* **24**, 521–538.
- KUEMMERER, H. 1978 Stability of laminar flows of micropolar fluids between parallel walls. *Phys. Fluids* **21**, 1688–1693.
- LIU, C. Y. 1970 On turbulent flow of micropolar fluids. *Intl J. Engng Sci.* **8**, 45–466.
- LIU, C. Y. 1971 Initiation of instability in micropolar fluids. *Phys. Fluids* **14**, 1808–1809.
- ŁUKASZEWICZ, G. 1999 Micropolar fluids. In *Theory and Applications, Modelling and Simulation in Science, Engineering and Technology*. Birkhäuser.
- ODENBACH, S. & GILLY, H. 1996 Taylor vortex flow of magnetic fluids under the influence of an azimuthal magnetic field. *J. Magn. Magn. Mater.* **152**, 123–128.
- PAPAUTSKY, I., BRAZZLE, J., AMMEL, T. & FRAZIER, A. B. 1999 Laminar fluid behaviour in microchannels using micropolar fluid theory. *Sens. Actuators* **73**, 101–108.
- PATEL, R., UPADHYAY, R. V. & MEHTA, R. V. 2003 Viscosity measurements of a ferrofluid: Comparison with various hydrodynamic equations. *J. Colloid Interface Sci.* **263**, 661–664.
- POPEL, A. S., REGIRER, S. A. & USICK, P. I. 1974 A continuum model of blood flow. *Biorheology* **11**, 427–437.

- ROSENTHAL, A. D., RINALDI, C., FRANKLIN, T. & ZAHN, M. 2004 Torque measurements in spin up flow of ferrofluids. *ASME Trans. J. Fluids Engng* **126**, 19–205.
- SASTRY, V. U. K. & DAS, T. 1985 Stability of Couette flow and Dean flow in micropolar fluids. *Intl J. Engng Sci.* **23**, 1163–1177.
- SHLIOMIS, M. I. 1972 Effective viscosity of magnetic suspensions. *Sov. Phys. JETP* **34** 129–1294.
- STOKES, V. K. 1984 *Theories of fluids with microstructure*, (Ch. 6), Springer-Verlag.
- TAYLOR, G. I. 1923 Stability of a viscous liquid contained between two rotating cylinders. *Phil. Trans. R. Soc. (Lond.) Ser. A* **223**, 289–343.
- VERMA, P. D. S. & SEHGAL, M. M. 1968 Couette flow of micropolar fluids. *Intl J. Engng Sci.* **6**, 23–238.
- WANG, X. L. & ZHU, K. Q. 2004 A study of the lubricating effectiveness of micropolar fluids in a dynamically loaded journal bearing (T1516). *Tribol. Intl* **37**, 481–490.
- WANG, X. L. & ZHU, K. Q. 2006 Numerical analysis of journal bearings lubricated with micropolar fluids including thermal and cavitating effects. *Tribol. Intl* **39**, 227–237.